Effects of Zinc Finger Protein A20 on Lipopolysaccharide (LPS)-Induced Pulmonary Inflammation/Anti-Inflammatory Mediators in an Acute Lung Injury/Acute Respiratory Distress Syndrome Rat Model

Authors' Contribution:
Study Design A
Data Collection B
Statistical Analysis C
Data Interpretation D
Manuscript Preparation E
Literature Search F
Funds Collection G

D 1 **Ding-Qian Wu**
E 1 **Hong-Bo Wu**
F 1 **Mao Zhang**
ABC 2 **Jian-An Wang**

1 Department of Emergency, The Second Affiliated Hospital of Zhejiang University School of Medicine, Hangzhou, Zhejiang, P.R. China
2 Department of Internal Medicine-Cardiovascular, The Second Affiliated Hospital of Zhejiang University School of Medicine, Hangzhou, Zhejiang, P.R. China

Corresponding Author: Jian-An Wang, e-mail: jiananwja@163.com
Source of support: This work was supported by Medical and Health Scientific Research Foundation of Zhejiang province (2017195219), China

Background: The aim of this study was to investigate the effects of zinc finger protein A20 on lipopolysaccharide (LPS)-induced pulmonary inflammation/anti-inflammatory mediators in an acute lung injury/acute respiratory distress syndrome (ALI/ARDS) rat model.

Material/Methods: Forty-eight ALI/ARDS rats were selected and assigned into normal saline (NS) (injected with NS), LPS (injected with LPS), LPS-C1 (injected with pEGFP-C1, NS and LPS), and A20 groups (injected with pEGFP-C1-A20, NS, and LPS). The wet/dry (W/D) ratio of rat lung tissues and total protein concentration and the number of neutrophils in bronchoalveolar lavage fluid (BALF) were detected. Enzyme-linked immunosorbent assay (ELISA) and qRT-PCR were applied to detect the protein and mRNA expressions of A20, IL-10, and TNF-α, respectively. Western blotting was employed to detect the protein expressions of A20, nuclear factor-kappa B (NF-κB) p65 and NF-κB p-P65 in rat lung tissues.

Results: Compared with the NS group, the W/D ratio of rat lung tissues and total protein concentration and the number of neutrophils in BALF in the other 3 groups increased significantly. The protein and mRNA expressions of A20, IL-10, and TNF-α were significantly higher in the LPS group than in the NS group. The protein and mRNA expressions of A20 and IL-10 were significantly up-regulated and the expression of TNF-α, NF-κB p65, and NF-κB p-P65 was significantly down-regulated in rats injected with A20 compared to those in the LPS group.

Conclusions: The study provided evidence that zinc finger protein A20 can alleviate pulmonary inflammation by inhibiting TNF-α, NF-κB p65, and NF-κB p-P65 expressions and promoting IL-10 expression.

MeSH Keywords: **Acute Lung Injury • Lipopolysaccharides • Myeloid-Lymphoid Leukemia Protein • Respiratory Distress Syndrome, Newborn**

Full-text PDF: http://www.medscimonit.com/abstract/index/idArt/901700

📄 3948   ▦ 3   📊 7   📖 29

Background

Acute lung injury/acute respiratory distress syndrome (ALI/ARDS) are life-threatening diseases which are characterized by acute lung inflammation leading to pulmonary congestion, hypoxemia, and decreased pulmonary compliance [1]. ALI/ARDS is the major cause of death in critical care, with a mortality rate of 40–60%, and they also contribute to a long-term illness and disability, with considerable pulmonary and psychological morbidity observed in 50% to 70% of survivors, and only 49% of them can return to employment by 1 year after discharge [2]. ARDS or ALI can be caused not only by primary lung disorders (such as pneumonia, aspiration, near-drowning, inhalation injuries, and contusions from trauma), but also by sepsis, burns, shock, and pancreatitis systemic disorders [3]. ALI/ARDS can lead to hypoxemia and diffuse bilateral infiltrates of the lung, usually followed by pulmonary edema, decreased lung compliance, and reduced functional residual capacity of the lung [4]. Lipopolysaccharide (LPS), the outer-membrane glycolipid component of gram-negative bacteria, is known for its powerful pro-inflammatory ability and for its potent capability to activate monocytic cells, which can induce ALI/ARDS [5,6]. New therapies for LPS-induced ALI/ARDS are urgently needed.

Zinc finger protein A20, also termed tumor necrosis factor (TNF)-α induced protein-3 (TNFAIP3), was first identified as a TNF-responsive gene in endothelial cells (ECs); it is expressed in a wide range of cells, such as B cells, T cells, and fibroblasts [7,8]. A20 plays an anti-inflammatory role and suppresses the expression of TNF-α to protect against liver injury, and A20 also has a dual cytoprotective function in ECs and hepatocytes [8,9]. As a soluble protein, TNF-α is associated with many human pathologies, and most biological effects of TNF-α are mediated via the appropriate associated receptor, which is related to the activation of nuclear factor-kappa B (NF-κB) pathway [10]. IL-10 is a cytokine which possesses anti-inflammatory properties, so it is able to limit pro-inflammatory responses and repress unnecessary tissue disruptions brought about by inflammation, giving it indispensable functions in various infectious and inflammatory diseases [11,12]. Previous studies have reported that TNF-α is the key inflammatory mediator participating in the progression of ALI/ARDS, while IL-10, as an anti-inflammatory cytokine, may provide protective effects against ALI/ARDS characterized by lung inflammation [13,14]. Because A20 is an important negative regulator of inflammation, we hypothesized that A20 has a close relationship with ALI/ARDS characterized by lung inflammation, and the possible mechanism is that A20 ameliorates ALI/ARDS by inhibiting pro-inflammatory TNF-α and increasing the expression of anti-inflammatory IL-10.

Material and Methods

Study subjects

A total of 48 healthy male Sprague-Dawley (SD) rats aged 5~6 weeks (150-180g) were selected. All rats were kept in a clean environment with a temperature of 22°C and a humidity of 49.7%. All experimental procedures were under the permission of the Animal Ethics Committee (AEC), and were in accordance with animal protection, animal welfare, and ethics principles, and conformed with national provisions for animal welfare and ethics.

Construction of zinc finger protein A20 expression plasmid

On the basis of the gene sequence of zinc finger protein A20, 5.0 Primer Design software was utilized to design primers with cleavage sites for restriction. The upstream primer was 5'-TCTAGATGCTGTACAAGTCCGGACTC-3' (Xba I cleavage sites), and the downstream primer was 5'-ACCGGATCTAGATAACTGATATCGGATCC-3' (BamH I cleavage sites). PCR amplification was conducted as follows: pre-denaturation at 94°C (10 min) and then 93°C (30 s), 54°C (30 s), and 72°C (105 s) for 35 cycles, followed by denaturation at 72°C for 10 min and preserved at 4°C. PCR product was detected by 1% agarose gel electrophoresis and the results were analyzed. PCR products were connected with vector pUC57 (Nanjing Kinross Biotechnology Co., Nanjing, China) and puc57-ha20 was transformed into *Escherichia coli* DH5α. A total of 5 single bacterial colonies were selected to perform PCR detection of bacteria. Corresponding bacterial colonies were chosen to carry out bacterial colonization on the basis of electrophoresis results. The High-purity Plasmid Mini Kit was utilized to purify plasmids after the expanding cultivation of bacterial strain, then the purified plasmid was sent to Nanjing Kinross Biotechnology Company to perform sequencing. The A20 gene fragment was then obtained after double-enzyme digestion of pUC57-hA20 plasmid with Xba I and BamH I. A20 gene fragment was then connected with eukaryotic expression plasmid (pEGFP-C1) after double-enzyme digestion with BamH I and Bgl II at 16°C overnight (vector sequences: PEGFP-C-5: CATGGTC-CTGCTGGAGTTCGTG). Positive colonies were screened from transformed *Escherichia coli* DH5α on a LB solid plate containing 50 g/ml ampicillin. Plasmid purification was conducted after amplification and double-enzyme identification with BamH I/Bgl II was performed on a small amount of recombinant DNA plasmid (pEGFP-C1-A20). Bacterial fluid was sent to Nanjing Kinross Biotechnology Company to conduct sequencing.

Grouping and processing

Forty-eight animals were randomly assigned into 4 groups (12 rats for each group). Injection was carried out on the basis of

ANIMAL STUDY

Table 1. The degree of pathological change in rat lung tissues.

Degree	Pathological change
0	Normal pulmonary vessels, alveolar, interstitial substance, and bronchial
I	Pulmonary interstitial edema, a small amount of inflammatory cells, and extent of edema and hemorrhage in interstitial substance and alveolar <25%
II	Inflammatory cells in the interstitial substance and part of the alveolar, alveolar septums were thickened, extravasation of blood in alveolar capillary and extent of edema and hemorrhage in alveolar between 25–50%
III	Inflammatory cells in the interstitial substance and most of the alveolar, alveolar septums were significantly thickened, extravasation of blood in alveolar capillary and extent of edema and hemorrhage in alveolar >50%

"gene transfection technique for rapid tail vein injection according to hemodynamics" established by Fu Liu et al. [15]. The 4 groups were as follows: the normal saline (NS) group: NS was injected into caudal vein within 5 s (1 mL for each rat); the LPS group: caudal vein of each rat was injected with 1 mL NS within 5 s and was injected with 10 mg/kg LPS (2 mg/ml) (Sigma-Aldrich Chemical Company, St Louis, MO, USA) 8 h later; the LPS-C1 group: 10 µg empty vector pEGFP-C1 and 1mL NS were injected into caudal vein of each rat within 5 s and l0 mg/kg LPS (2 mg/ml) was injected 8 h later; and the A20 group: 10 µg pEGFP-C1-A20 and 1mL NS were injected into caudal vein of each rat within 5 s and was then injected with 10 mg/kg LPS (2 mg/ml) 8 h later. Twenty-four hours after the injection of NS or LPS, the rats in the NS group and rats in other groups were anesthetized with urethane (ethyl carbonate) (7.5 ml/kg). Celiac artery blood was collected and all rats were sacrificed. Samples were collected for follow-up experiments.

Detection of wet/dry (W/D) ratio in rat lung tissues and total protein concentration and the number of neutrophils in bronchoalveolar lavage fluid (BLAF)

After the rats were sacrificed, the thoracic cavity was quickly opened and the right primary bronchus was litigated. The superior lobe of the right lung was removed and put on an electronic balance to measure wet weight, and then was put into an incubator at 60°C for 48 h until the weight showed no change to measure dry weight. The W/D ratio was calculated to evaluate the degree of pulmonary edema.

We obtained BLAF from the left lung tissues of rats. The left lung was injected with 1×PBS 2 mL via the trachea cannula and the drawing-in was repeated 3 times, followed by BALF recycling. BALF was centrifuged at 4°C at 1200 rpm for 14 min to collect supernatant. To observe the protein exudation in rat alveoli, bovine serum albumin (BSA) standard solution and working solution were prepared according to the instructions of the Bicinchoninic Acid (BCA) Protein Assay Kit (Thermo Fisher Scientific, CA, USA). The 15-µL/well standard solution and BLAF were put into a microwell plate, shaken,

and incubated at 37°C for 30 min. After cooling to room temperature, a semi-automatic biochemical analyzer (Shanghai Biochemical Analysis Instrument Co., Ltd., Shanghai, China) was used to measure optical density (OD) values per well and calculate the total protein content at the wavelength of 562 nm. To detect the alveolar neutrophil infiltration of rats, BALF was centrifuged at 4°C at 1200 rpm for 10 min, and then the supernatant was discarded. The cells were resuspended in 0.5 mL phosphate-buffered saline (PBS) for precipitation, and 10 µL was collected to count for neutrophils.

Light microscopy observation

The inferior lobe of the right lung was quickly removed from killed rats and fixed in 4% poly-formaldehyde for 24 h. The tissues were dehydrated with 70%, 90%, 95%, and 100% graded doses of alcohol. Then, the inferior lobe of the right lung was soaked in cedar oil overnight, waxed, and then embedded in paraffin wax. The paraffin block was cut into slices (5 µm), pasted, and toasted at 37°C. Those slices were dewaxed with dimethylbenzene 3 times and dehydrated with graded doses of alcohol. The slices were dried and stained with conventional hematoxylin-eosin (HE) for 10–20 min. Then, the slices were observed under a microscope after dewaxing, dehydration, and mounting. The degree of pathological change was scored (Table 1).

Enzyme-linked immunosorbent assay (ELISA)

Left lung tissues (150–200 mg) obtained from killed rats were washed with 4°C pre-cooled NS and dried with absorbent paper. Ophthalmic scissors were used to cut tissues as soon as possible, followed by the addition of 9-fold tissue homogenate medium. An ultrasonic homogenizing machine (Beijing HeDe Biotechnology Co., Ltd., Beijing, China) was used to homogenize tissues for 20 s and refrigerated centrifuge was then used at 3000 rpm at 4°C. The supernatant was identified as lung tissue homogenate and was put into 1.5-ml Ep tubes separately, and preserved in a freezer at −78°C. The whole homogenizing process was carried out on crushed ice. ELISA plates (Shanghai

Table 2. Premier sequences for qRT-PCR.

Gene	Premier sequence
A20	Upstream: 5'-GCAGTGTAAAAGGCAGGCTAAC-3'
	Downstream: 5'-TGGGGTTCTCTCTCGTATCTTC-3'
IL-10	Upstream: 5'-AACATACTGCTAACCGACTC-3'
	Downstream: 5'-TGGCCTTGTAGACACCTT-3'
TNF-α	Upstream: 5'-TACTGAACTTCGGGGTGATTGGTC C- 3'
	Downstream: 5'-CAGCCTTGTCCCTTGAAGAGAACC-3'
β-actin	Upstream: 5'-GATTGCCTCAGGACATTTCTG-3'
	Downstream: 5'-GATTGCTCAGGACAT TTCTG-3'

qRT-PCR – quantitative real-time polymerase chain reaction.

Alpha Biotechnology Co., Ltd., Shanghai, China) were washed with deionized water 3 times and then dried after soaking in the deionized water overnight. Homogenizing supernatant (10 µl/well) and diluted solution (50 µl/well) were coated at 4°C overnight and then washed with poly (butylene succinate-co-terephthalate) (PBST) 3 times. After the addition of 1% BSA (60 µl/well), the solution was sealed at 37°C for 1 h and then washed with PBST 3 times. Mouse anti-human A20 monoclonal antibody were added into the solution at 75 µl/well with a dilution of 1: 2500 (Active Motif Inc., Carlsbad, CA, USA) at 37°C for 1 h and washed with PBST 3 times. Then, 10 µl sheep anti-mouse IgG-HRP (Beijing North TZ-Biotech Develop., Co. Ltd) was added to each well with a dilution of 1: 7500, incubated at 37°C for 1 h, and washed with PBST 3 times. Each well received 1 drop of color developing solution A and 1 drop of color developing solution B (Shanghai Alpha Biotechnology Co., Ltd., Shanghai, China) and the coloration process lasted for 10 min. The reaction was terminated by adding 2 mo1/L H_2SO_4 (Shanghai Alpha Biotechnology Co., Ltd., Shanghai, China). Color comparator was used to measure the OD_{540nm} value. An ELISA kit used to separately pack IL-10 and TNF-α was purchased from Wuhan Boster Biological Engineering Co., Ltd. (Wuhan, China) and we followed the manufacturer's instructions.

Quantitative real-time polymerase chain reaction (qRT-PCR)

Lung tissues (about 100 mg) were cut in a plate placed on ice and 1 mL extracting RNA (TRIZOL reagent, Invitrogen Inc., Carlsbad, CA, US) was added and performed with repeated aspiration to obtain an emulsion. After the addition of 200 µL chloroform, the solution was quickly shaken for 15 s and placed at room temperature for 5 min. The tissue samples were then centrifuged at 13 000 rpm at 49°C for 15 min and the obtained supernatant was added to 500 µL dimethyl carbinol and precipitated on ice for 1 h. The supernatant was discarded and the precipitation was washed with 75%

alcohol and the centrifugation was repeated. Finally, moderate diethyl phosphorocyanidate (DEPC) was used to dispose the precipitation of water-soluble RNA and extract total RNA. cDNA was obtained from 20 µL reverse transcription reaction system. The cDNA (3 µ1), DEPC water, buffer solution, dNTPs, Taq DNA polymerase, and primers were then added into the 25 µ1 reaction system for reaction in PCR amplification instrument (USA model: PTC-100TM, MJ Research Inc., Watertown, MA). Amplification conditions were as follows: denaturation at 94°C for 3 min, annealing at 56°C for 30 min, extension at 72°C for 8 min, and cycling 35 times. PCR products were conducted with 2% agarose gel electrophoresis and ID image analysis software (Eastman Kodak Company, Rochester, NY, USA) was applied for the band analysis. Relative expressions of mRNA of detected specimens = the absorbance of amplified products to be tested/the absorbance of amplified products obtained from the β-actin-specific primers. The relative quantity of target genes was $2^{-\Delta\Delta Ct}$ [16]. ΔCT=the domain value of the target gene – the domain value of β-actin. ΔΔCT=the group to be tested (CT_{target} – $CT\beta_{-actin}$) – the standard group (CT_{target} – $CT\beta_{-actin}$). The primer sequences of A20, TNF-α, IL-10, and β-actin were shown in Table 2.

Western blotting

Lung tissue homogenate were taken out for the detection of total protein concentration using a BCA Protein Quantitation kit (Pierce, Rockford, IL). Based on the samples with minimum concentration, other samples were adjusted to the same concentration and 5×SDS sample buffer of the same volume were added. The samples were mixed using vortex oscillation and denaturation at 100°C for 5–10 min. Then, the samples were conducted with sodium dodecyl sulfate-polyacrylamide gel electrophoresis (SDS-PAGE), transferred to membrane, sealed, and incubated with primary antibody (Rabbit anti-mouse A20, nuclear factor-kappa B (NF-κB) p65, NF-κB p-P65 and GAPDH antibody, R&D Systems, Minneapolis, MN, USA), at 4°C overnight.
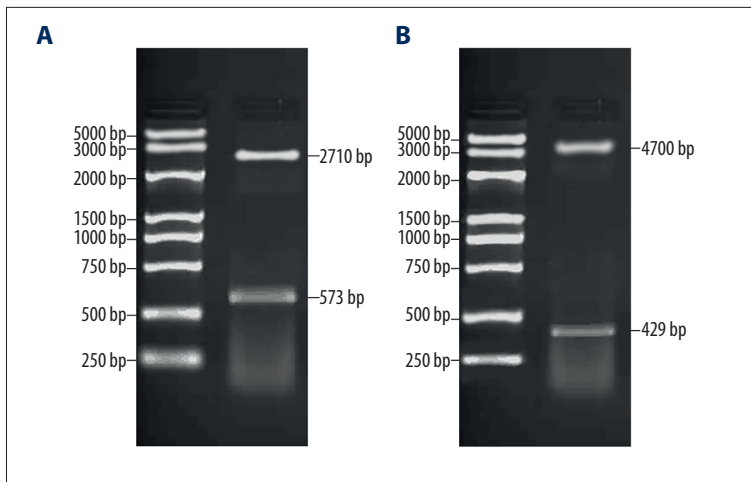
Figure 1. Double-enzyme digestion and identification of vector pEGFP-C1-A20. (**A**) Double-enzyme digestion of A20 pUC57 plasmid; M, Marker; I, double-enzyme digestion of Xba I/BamH I; (**B**) Double-enzyme digestion of A20 pEGFP-C1 plasmid; M – Marker; I – double-enzyme digestion of BamH1/Bgl II.

After membrane cleaning, the samples were incubated with secondary antibody at room temperature for 1 h. Then, the cleaning was performed for 10 min repeated 3 times, and detected by electrogenerated chemiluminescence (ECL).

Statistical analysis

Results are displayed as mean ± standard deviation ($\overline{\chi}$±s). All data were analyzed by SPSS 21.0 software (SPSS, Inc, Chicago, IL, USA). One-way analysis of variance (ANOVA) was utilized to compare data among multiple groups, and the comparisons between 2 groups were conducted by Student's t-test ($P<0.05$ set as a standard to show significance). $P<0.05$ represented that the difference is significant.

Results

Construction and identification of vector pEGFP-C1-A20

pUC57-A20 plasmid was obtained after the connection of PCR product of zinc finger protein A20 gene and pUC57 plasmid. Double-enzyme digestion was performed on the recombinant plasmid, vector pUC57 was removed, and a 573 bp insertion sequence, which was in accordance with the design fragment, was obtained. Then, the A20 target fragment was connected with vector pEGFP-C1 to construct the recombinant pEGFP-C1-A20 plasmid, and the actual length was in accordance with the design length (Figure 1).

Comparisons of the W/D ratio in rat lung tissues and total protein concentration and the number of neutrophils in BLAF among 4 groups

The W/D ratios of rat lung tissues indicate the lung water content. The results were as follows. Compared with the W/D ratio of rat lung tissues in the NS group (4.30±0.41), the W/D ratio in

the LPS group (5.58±0.53), the LPS-C1 group (5.55±0.52), and the A20 group (4.87±0.46) were clearly increased (all $P<0.05$); however, the W/D ratio in the A20 group declined significantly more than in the LPS group ($P<0.05$). Total protein concentration in BLAF was also detected to reflect the alveolar-capillary membrane permeability. The total protein concentration in BLAF in the LPS group (348.50±17.42), the LPS-C1 group (345.18±17.26 µg/ml) and the A20 group (315.31±15.76) increased markedly more than in the NS group (214.22±10.71); however, the total protein concentration in BLAF in the A20 group was clearly down-regulated compared to the LPS group ($P<0.05$). The alveolar neutrophil infiltration was also detected, and the results were as follows: compared with the NS group (28.00±5.46), the LPS group (326.00±11.75), the LPS-C1 group (295.50±17.71) and the A20 group (161.91±14.48) had elevated neutrophil counts, while compared with the LPS and LPS-C1 groups, the A20 group had significantly down-regulated neutrophil counts ($P<0.05$) (Figure 2).

Comparisons of HE staining of rat lung tissues after injection among 4 groups

The pathological changes of rat lung tissues were observed. The alveolus of the rats in the NS group was complete, and there was no edema in the alveolar wall and no obvious inflammatory cell infiltration in the lung. No significant difference between the LPS group and the LPS-C1 group was observed, and in both groups alveolar septums were thickened, and inflammatory cell infiltration and red blood cell and neutrophil exudation at the alveolar cavity were observed; a large number of red blood cell and neutrophil exudation at the cell gap of lung tissues were observed; the degree of inflammation in the A20 group was lower than that in the LPS and LPS-C1 groups, edema and inflammatory infiltration of lung tissues also decreased in the A20 group (Figure 3). The degree of pathological change in rat lung tissues was scored and is shown in Table 3.
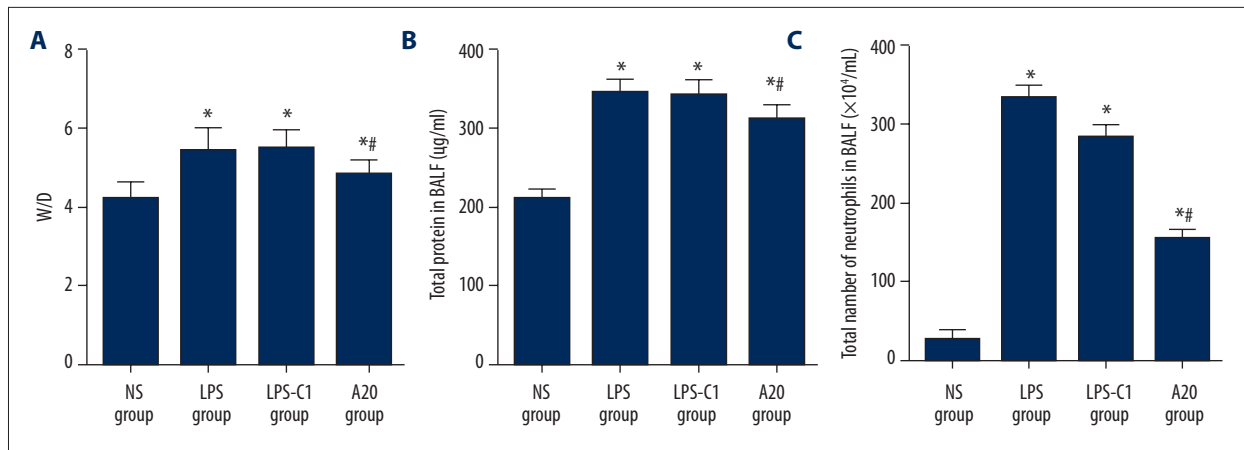
Figure 2. Comparisons of W/D ratio in rat lung tissues and total protein concentration and the number of neutrophils in BLAF among 4 groups. (**A**) W/D ratio in rat lung tissues; (**B**) total protein concentration in BLAF (µg/mL); (**C**) the number of neutrophils in BLAF; BLAF – bronchoalveolar lavage fluid; NS – normal saline; LPS – lipopolysaccharide; C1 – pEGFP-C1; * $P<0.05$ compared with the NS group; # $P<0.05$ compared with the LPS group; Experimental data are presented as mean ± standard deviation (SD); n=12.
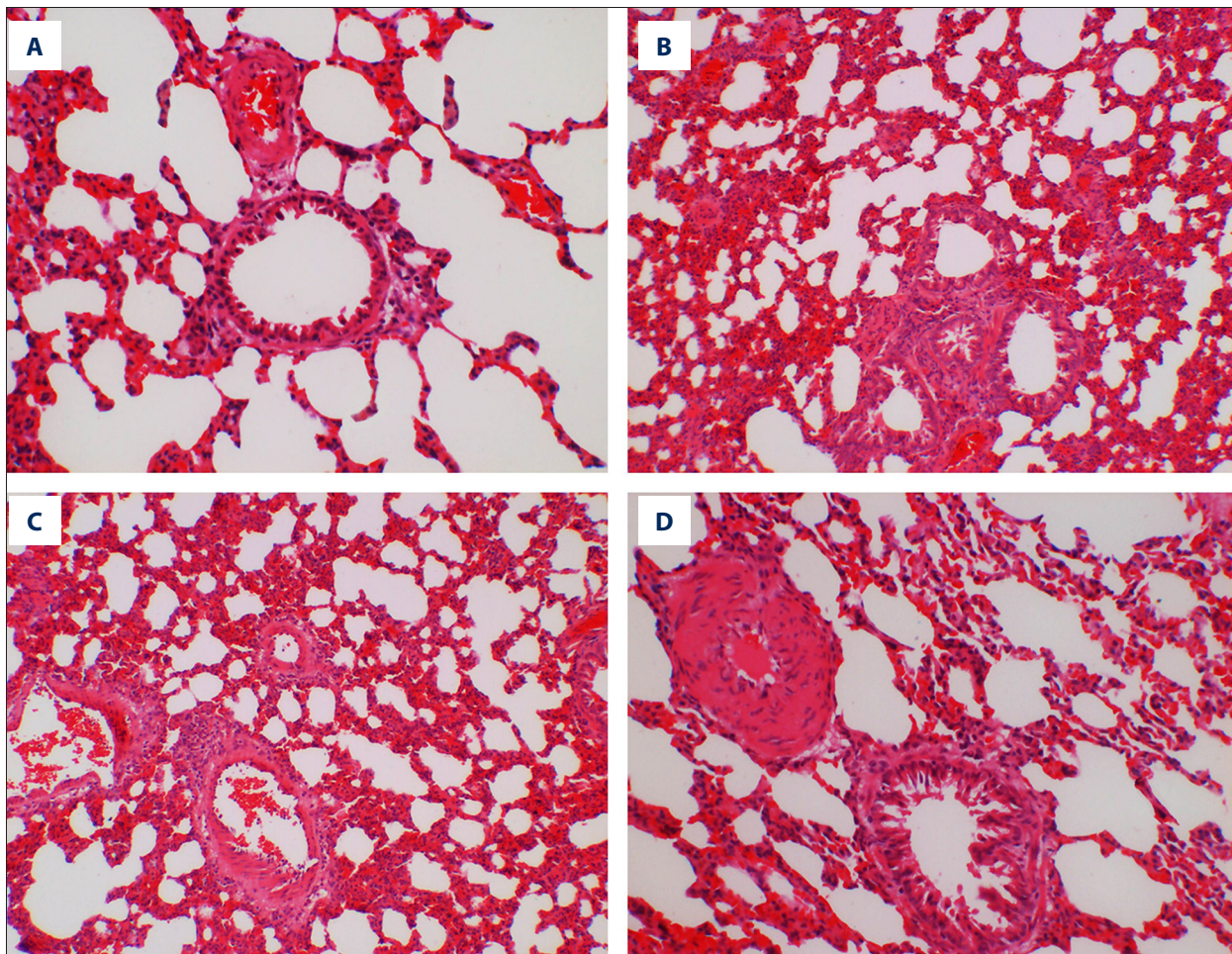

Figure 3. HE staining images of rat left lung tissues 24 h after injection with NS or LPS among 4 groups (400× magnification). NS – normal saline; LPS – lipopolysaccharide; C1 – pEGFP-C1; (**A**) the NS group; (**B**) the LPS group; (**C**) the LPS-C1 group; (**D**) the A20 group; n=12.

Table 3. The degree of pathological change in rat lung tissues.

Degree	N	0	I	II	III	Ridit value
NS group	12	12	0	0	0	0
LPS group	12	0	4	8	0	0.83*
LPS-C1 group	12	0	5	7	0	0.88*#
A20 group	12	0	7	5	0	0.86*#

* $P<0.05$ compared with the NS group; # $P<0.05$ compared with the LPS group; N – number; NS – normal saline;
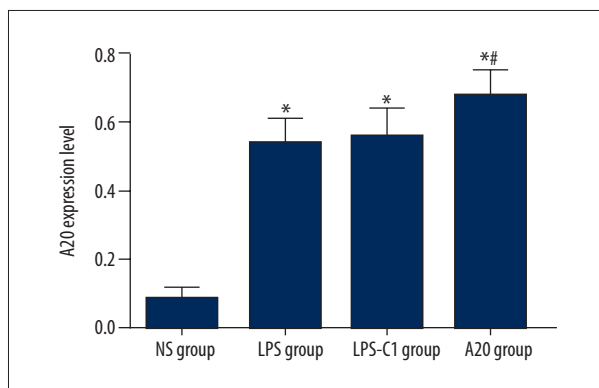LPS – lipopolysaccharide; C1 – pEGFP-C1.

Figure 4. Comparisons of zinc finger protein A20 expression in rat lung tissues 24 h after injection among 4 groups. NS – normal saline; LPS – lipopolysaccharide; C1 – pEGFP-C1; * $P<0.05$ compared with the NS group; # $P<0.05$ compared with the LPS group; n=12.

Comparisons of zinc finger protein A20 expression in rat lung tissues after injection among 4 groups

Compared with the NS group, the expression of A20 was significantly higher in the LPS group, the LPS-C1 group, and the A20 group (all $P<0.05$), indicating that LPS could induce the expression of zinc finger protein A20 in lung tissues. The expression of A20 was significantly elevated in the A20 group compared to the LPS group and the LPS-C1 group ($P<0.05$), indicating that vector pEGFP-C1-A20 was successfully transfected into the experimental rats to synthetize zinc finger protein A20. No significant difference was found in the expression of A20 between the LPS group and the LPS-C1 group ($P>0.05$) (Figure 4).

Comparisons of IL-10 and TNF-α expressions in rat lung tissues after injection among 4 groups

IL-10 expression in rat lung tissues increased significantly in the LPS group, the LPS-C1 group, and the A20 group compared to the NS group ($P<0.05$), and the A20 group presented
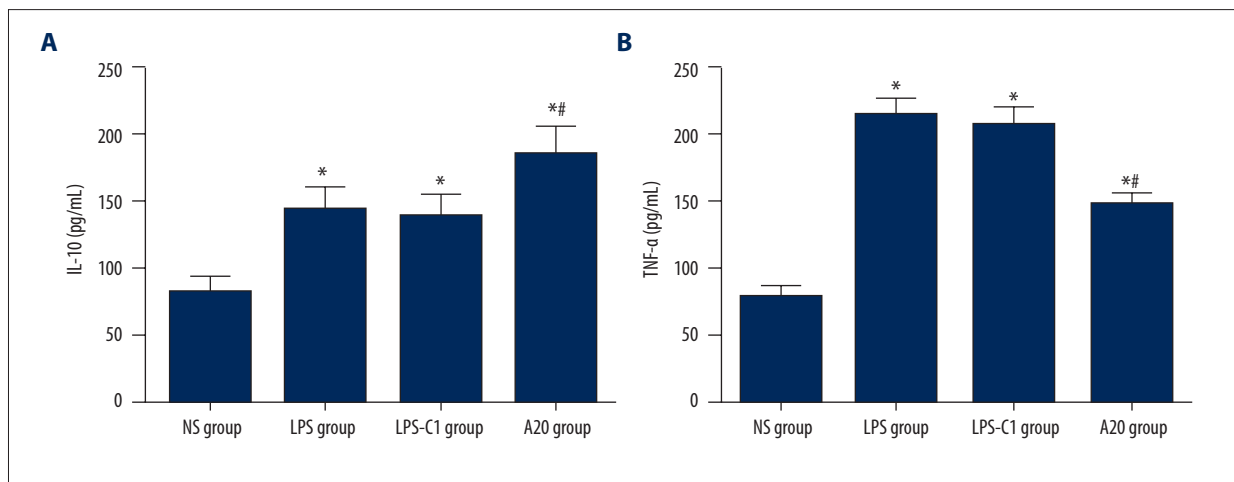

Figure 5. Comparisons of IL-10 (A) and TNF-α (B) expressions in rat lung tissues 24 h after injection with NS or LPS among 4 groups. NS – normal saline; LPS – lipopolysaccharide; C1 – pEGFP-C1; * $P<0.05$ compared with the NS group; # $P<0.05$ compared with the LPS group; n=12.
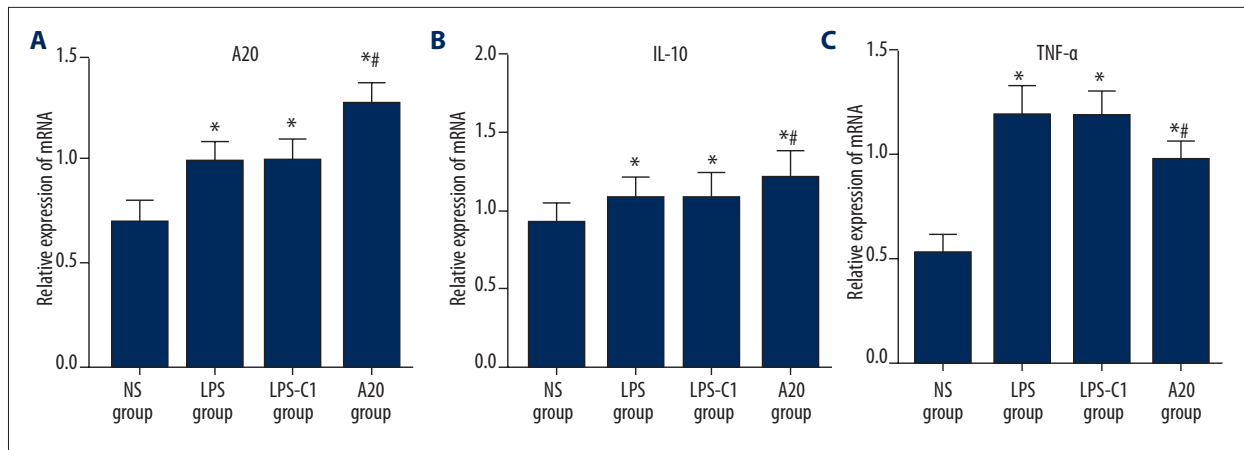
Figure 6. (**A–C**) Comparisons of relative mRNA expressions of A20, TNF-α, and IL-10 in rat lung tissues among 4 groups. NS – normal saline; LPS – lipopolysaccharide; C1 – pEGFP-C1; [#] $P<0.05$ compared with the LPS group, n=12.

significantly higher expression of IL-10 than in the LPS group and the LPS-C1 group ($P<0.05$), indicating that high expression of A20 could up-regulate the release of IL-10 to a certain degree. The expression of TNF-α in rat lung tissues was significantly lower in the NS group compared with that in the LPS, LPS-C1, and A20 groups ($P<0.05$); the expression of TNF-α in rat lung tissues declined markedly in the A20 group compared to the LPS group and the LPS-C1 group, indicating that high expression of A20 could down-regulate the release of TNF-α to a certain degree (Figure 5).

Comparisons of mRNA expressions of A20, TNF-α, and IL-10 in rat lung tissues after injection among 4 groups

The mRNA expression of A20 was significantly elevated in the LPS group, the LPS-C1 group, and the A20 group compared to the NS group; the A20 group exhibited higher mRNA expression of A20 than the LPS group and the LPS-C1 group (all $P<0.05$) (Figure 6A). The mRNA expression of IL-10 was significantly up-regulated in the LPS, LPS-C1, and A20 groups compared to the NS group; the A20 group showed increased expression of IL-10 compared to the LPS group and the LPS-C1 group (all $P<0.05$) (Figure 6B). The mRNA expression of TNF-α increased significantly in the LPS group, the LPS-C1 group and the A20 group compared to the NS group; the A20 group presented decreased expression of TNF-α compared to the LPS group and the LPS-C1 group (all $P<0.05$) (Figure 6C).

Comparisons of protein expressions of A20, NF-κB p65, and NF-κB p-P65 in rat lung tissues among 4 groups

The A20 group exhibited significantly up-regulated A20 expression compared to the NS, LPS, and LPS-C1 groups, and down-regulated NF-κB p65 and NF-κB p-P65 expression compared to the LPS and LPS-C1 groups, indicating that the high protein expression of A20 can inhibit the expression of NF-κB
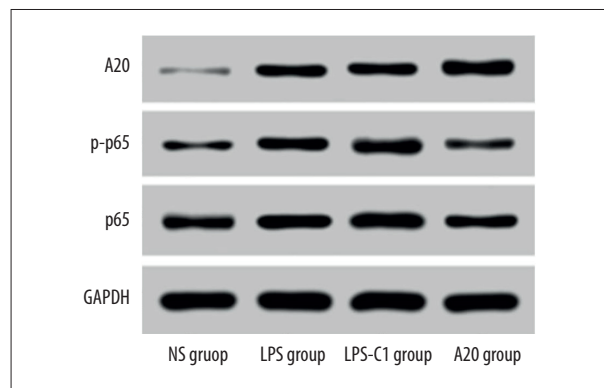

Figure 7. Comparisons of protein expressions of A20, NF-κB p65, and NF-κB p-P65 in rat lung tissues among 4 groups. NS – normal saline; LPS – lipopolysaccharide; C1 – pEGFP-C1.

p65 and NF-κB p-P65 to some extent, thus influencing the NF-κB signaling pathway (Figure 7).

Discussion

ALI/ARDS are syndromes of acute respiratory failure which occur as a series of malignancy attributed to diverse risk factors [17]. In spite of the advances in therapeutic principles and surgical techniques, ALI/ARDS still have high incidence and poor outcome, and ALI/ARDS continues to be a leading cause of morbidity and mortality in humans [18]. A20, known for many years as an anti-apoptotic protein through inhibiting the NF-κB signaling pathway, received attention in recent studies as an important negative regulator of inflammation [19]. Therefore, the present study aimed to elucidate the role and mechanism of A20 in pulmonary inflammation in an ALI/ARDS rat model.

Initially, our study revealed that the W/D ratio of rat lung tissues and total protein concentration and the number of neutrophils in BALF were significantly reduced in the A20 group compared to the LPS group. LPS is one of the main components of gram-negative bacteria cell walls, and upon infection with LPS, an activation of the inflammatory cascade leading to the release of inflammatory mediators is involved in the occurrence and progression of ALI/ARDS [20]. The W/D ratio was calculated as an indicator of lung edema, and LPS has been reported to be able to elevate the total protein concentration in BALF; however, A20 can inhibit the increased concentration of inflammatory cells in BALF induced by LPS through down-regulating the NF-κB signaling pathway, so the W/D ratio of rat lung tissues and total protein concentration in BALF were significantly decreased in the A20 group compared to the LPS group [13,21]. Neutrophil infiltration into the alveolar space causes lung injury; hence, neutrophil depletion plays a protective role in ALI [22]. Previous research also demonstrated that activation of NF-κB reduces neutrophil apoptosis of lungs in ALI patients [23]. The possible mechanism by which LPS induces ALI/ARDS is that LPS activates the NF-κB signaling pathway to increase the expressions of many cytokines, including TNF-α [24]. However, A20 has been extensively reported to be a potent inhibitor of activation of the NF-κB signaling pathway. A20 regulates TNF-mediated NF-κB activation by functioning as a dual ubiquitin-editing enzyme. TNF and LPS trigger the phosphorylation of A20 at the site of Ser[381], which, by a currently undetermined mechanism, improves the ability of A20 to inhibit the NF-κB signaling pathway [25]. Another laboratory study revealed that A20 null mice fail to block TNF-induced NF-κB activation, develop serious inflammation, and die quickly, indicating the important role of A20 in anti-inflammatory processes [26]. Therefore, it is reasonable to speculate that LPS increases the expression of A20, and the accumulated expression of A20 results in the blockade of NF-κB signaling pathway, repressed sensitivity of LPS in rats, and alleviated progression of ALI/ARDS.

In addition, we found that the protein and mRNA expressions of A20, IL-10, and TNF-α were significantly elevated in the LPS group compared to the NS group. It is becoming increasingly evident that inflammatory mediators play important roles in the pathogenesis and development of ALI/ARDS; therefore, the identification of the key cytokines in ALI/ARDS coupled with the investigation of potent inhibitors would make it possible to develop anti-inflammatory therapy with significant clinic efficacy [27]. TNF-α is known as an elevated pro-inflammatory cytokine in ALI/ARDS that can stimulate the production of other cytokines, while IL-10 is a highly potent anti-inflammatory cytokine that can prevent macrophages from producing cytokine, and the ratio of concentrations of TNF-α/IL-10 has been reported to be significantly increased in ALI/ARDS patients [28].

Furthermore, our study demonstrated that the high protein expression of A20 can inhibit the expression of NF-κB p65, thus influencing the NF-κB signaling pathway. Our previous research has clearly established the role of A20 in the negative regulation of inflammation via suppressing the activity of the NF-κB signaling pathway, resulting in the downregulation of pro-inflammatory TNF-α and the up-regulation of anti-inflammatory IL-10 [29]. The balance between pro- and anti-inflammatory cytokines in the lungs of ALI/ARDS patients is a key step toward understanding the pathogenesis of the devastating disease and helping in the development of clinical strategies to reduce the clinical severity and mortality of ALI/ARDS, and A20 is a potent regulator of this balance [28].

Conclusions

In conclusion, our study clarifies that LPS, IL-10, TNF-α can increase the expression of A20 in a rat model, and the elevated expression of A20 can inhibit the sensitivity of LPS in rats and alleviate ALI/ARDS. Moreover, A20 represses inflammation by promoting the expression of anti-inflammatory IL-10 and inhibiting the expression of inflammatory TNF-α. Therefore, enhancing the expression of A20 may be a promising therapeutic strategy in treating inflammatory autoimmune diseases. However, the effects of A20 on other organs and other inflammatory mediators have yet to be clarified.

Competing interests

None.

References:

1. Sud S, Sud M, Friedrich JO et al: High frequency oscillation in patients with acute lung injury and acute respiratory distress syndrome (ARDS): Systematic review and meta-analysis. BMJ, 2010; 340: (c2327

2. Hayes M, Curley G, Ansari B et al: Clinical review: Stem cell therapies for acute lung injury/acute respiratory distress syndrome – hope or hype? Crit Care, 2012; 16(2): 205

3. Prabhakaran P: Acute respiratory distress syndrome. Indian Pediatr, 2010; 47(10): 861–68

4. Perl M, Lomas-Neira J, Venet F et al: Pathogenesis of indirect (secondary) acute lung injury. Expert Rev Respir Med, 2011; 5(1): 115–26

5. Wang HQ, Meng X, Liu BQ et al: Involvement of JNK and NF-kappaB pathways in lipopolysaccharide (LPS)-induced BAG3 expression in human monocytic cells. Exp Cell Res, 2012; 318(1): 16–24

6. Zeng Z, Gong H, Li Y et al: Upregulation of miR-146a contributes to the suppression of inflammatory responses in LPS-induced acute lung injury. Exp Lung Res, 2013; 39(7): 275–82

7. Tang YJ, Zhang RZ, Liu XM et al: Effect of the topical application of calcipotriol on the expression levels of zinc finger protein A20 and nuclear factor-kappaB in the skin lesions of patients with psoriasis vulgaris. Exp Ther Med, 2016; 11(1): 247–50

8. Yang J, Xu MQ, Yan LN et al: Zinc finger protein A20 protects rats against chronic liver allograft dysfunction. World J Gastroenterol, 2012; 18(27): 3537–50

9. Liu B, Jiang D, Ou Y et al: An anti-inflammatory role of A20 zinc finger protein during trauma combined with endotoxin challenge. J Surg Res, 2013; 185(2): 717–25

10. Burke SJ, Lu D, Sparer TE et al: Transcription of the gene encoding TNF-alpha is increased by IL-1beta in rat and human islets and beta-cell lines. Mol Immunol, 2014; 62(1): 54–62

11. Saraiva M, O'Garra A: The regulation of IL-10 production by immune cells. Nat Rev Immunol, 2010; 10(3): 170–81

12. Ouyang W, Rutz S, Crellin NK et al: Regulation and functions of the IL-10 family of cytokines in inflammation and disease. Annu Rev Immunol, 2011; 29: 71–109

13. Zhang Y, Liang D, Dong L et al: Anti-inflammatory effects of novel curcumin analogs in experimental acute lung injury. Respir Res, 2015; 16: 43

14. Huang HL, Yang WY, Pu HF et al: Kruppel-like factor 5 associates with melamine-cyanurate crystal-induced nephritis in rats. Nephrol Dial Transplant, 2013; 28(10): 2477–83

15. Liu F, Song Y, Liu D: Hydrodynamics-based transfection in animals by systemic administration of plasmid DNA. Gene Ther, 1999; 6(7): 1258–66

16. Livak KJ, Schmittgen TD: Analysis of relative gene expression data using real-time quantitative PCR and the 2(-Delta Delta C(T)) Method. Methods, 2001; 25(4): 402–8

17. Luh SP, Chiang CH: Acute lung injury/acute respiratory distress syndrome (ALI/ARDS): the mechanism, present strategies and future perspectives of therapies. J Zhejiang Univ Sci B, 2007; 8(1): 60–69

18. Zhu YG, Qu JM, Zhang J et al: Novel interventional approaches for ALI/ARDS: Cell-based gene therapy. Mediators Inflamm, 2011; 2011: 560194

19. Catrysse L, Vereecke L, Beyaert R et al: A20 in inflammation and autoimmunity. Trends Immunol, 2014; 35(1): 22–31

20. Li Y, Wu R, Tian Y et al: RAGE/NF-kappaB signaling mediates lipopolysaccharide induced acute lung injury in neonate rat model. Int J Clin Exp Med, 2015; 8(8): 13371–76

21. Wang J, Ouyang Y, Guner Y et al: Ubiquitin-editing enzyme A20 promotes tolerance to lipopolysaccharide in enterocytes. J Immunol, 2009; 183(2): 1384–92

22. Wolthuis EK, Vlaar AP, Hofstra JJ et al: Plasminogen activator inhibitor-type I gene deficient mice show reduced influx of neutrophils in ventilator-induced lung injury. Crit Care Res Pract, 2011; 2011: 217896

23. Kupfner JG, Arcaroli JJ, Yum HK et al: Role of nf-kappab in endotoxemia-induced alterations of lung neutrophil apoptosis. J Immunol, 2001; 167(12): 7044–51

24. Ni YF, Wang J, Yan XL et al: Histone deacetylase inhibitor, butyrate, attenuates lipopolysaccharide-induced acute lung injury in mice. Respir Res, 2010; 11: 33

25. Coornaert B, Carpentier I, Beyaert R: A20: Central gatekeeper in inflammation and immunity. J Biol Chem, 2009; 284(13): 8217–21

26. Daniel S, Arvelo MB, Patel VI et al: A20 protects endothelial cells from TNF-, Fas-, and NK-mediated cell death by inhibiting caspase 8 activation. Blood, 2004; 104(8): 2376–84

27. Morty RE, Eickelberg O, Seeger W: Alveolar fluid clearance in acute lung injury: What have we learned from animal models and clinical studies? Intensive Care Med, 2007; 33(7): 1229–40

28. Goodman RB, Pugin J, Lee JS et al: Cytokine-mediated inflammation in acute lung injury. Cytokine Growth Factor Rev, 2003; 14(6): 523–35

29. Evans PC, Ovaa H, Hamon M et al: Zinc-finger protein A20, a regulator of inflammation and cell survival, has de-ubiquitinating activity. Biochem J, 2004; 378(Pt 3): 727–34